

Received September 15, 2020, accepted September 27, 2020, date of publication September 30, 2020, date of current version October 12, 2020.

Digital Object Identifier 10.1109/ACCESS.2020.3027854

Finite-Time Adaptive Fuzzy Quantized Control for a Quadrotor UAV

WEI YANG¹, GUOZENG CUI^{1,2}, JINPENG YU², CHONGBEN TAO^{1,3}, AND ZE LI¹, (Member, IEEE)

¹School of Electronic and Information Engineering, Suzhou University of Science and Technology, Suzhou 215009, China

²School of Automation, Qingdao University, Qingdao 266071, China

³Suzhou Automobile Research Institute, Tsinghua University, Suzhou 215134, China

Corresponding authors: Guozeng Cui (guozengcui@gmail.com) and Ze Li (lizeing@163.com)

This work was supported in part by the National Natural Science Foundation of China under Grant 61703059, Grant 61973179, Grant 61873144, and Grant 61801323; in part by the Natural Science Foundation of Jiangsu Province under Grant BK20170291, in part by the Taishan Scholar Special Project Fund under Grant TSQN20161026, in part by the China Post-Doctoral Science Foundation under Grant 2018M632621, in part by the Postgraduate Research and Practice Innovation Program of Jiangsu Province under Grant SJCX20_1111, in part by the Science and Technology Projects Fund of Suzhou under Grant SYG201708 and Grant SS2019029, in part by the Construction System Science and Technology Fund of Jiangsu Province under Grant 2017ZD066, in part by the Open Foundation of The Suzhou Smart City Research Institute, Suzhou University of Science and Technology, under Grant SZSCR2019003 and Grant SZSCR2019009, and in part by the Applied Research Project for Postdoctoral Researchers of Qingdao.

ABSTRACT In this paper, a finite-time command filtered backstepping (FTCFB) adaptive trajectory tracking control strategy is proposed for a quadrotor unmanned aerial vehicle (UAV) with quantized inputs and external disturbances. For the position subsystem and attitude subsystem, a finite-time command filter is introduced to faster approximate the derivative of virtual control signal, which can effectively avoid the problem of explosion of complexity inherent in the traditional backstepping design procedure. The fractional order error compensation mechanism is designed to remove the filter error, and it further improves control performance. From the Lyapunov stability theory, the boundedness of all signals in the closed-loop system is rigorously proved, and the position and attitude tracking errors can converge to a small neighborhood of the origin in finite-time. Finally, a numerical example is conducted to intuitively show the validity of the developed control scheme.

INDEX TERMS Quadrotor unmanned aerial vehicle, command filtered backstepping, adaptive quantized control, finite-time control.

I. INTRODUCTION

In the past decades, the quadrotor unmanned aerial vehicle (UAV) has attracted considerable attention due to its simple structure, efficient deployment, flexible maneuverability etc, and various practical applications have been reported such as aerial photography, urban fire rescue, cargo transportation and so on. However, on the account of the structure uncertainties and strong coupling nonlinear characteristics of quadrotor UAV [1]–[4], it is difficult to design an accurate trajectory tracking control scheme to achieve high quality flight.

In order to improve the control performances of quadrotor UAV, various advanced control algorithms such as sliding-mode control [5]–[7], fuzzy and neural networks-based

intelligent control [8]–[10] and backstepping-based adaptive control [11]–[13] have been proposed, respectively. By combining the tracking differentiator and extended state observer strategies, the issue of attitude tracking control for quadrotor UAV was solved in [14]. Note that the above-mentioned adaptive backstepping control algorithms might have a shortcoming “explosion of complexity” caused by the repeated derivatives of virtual control signals. Fortunately, the dynamic surface control (DSC) technique, which was firstly proposed in [15], was established to avoid “explosion of complexity” by introducing a first-order filter for virtual control signals. Subsequently, many researchers focused on developing the trajectory tracking control schemes of quadrotor UAV based on DSC technique, see [16]–[20] and references therein. In [18], adaptive DSC algorithm was proposed under time-varying output constraints and model uncertainties. The adaptive prescribed performance DSC scheme was

The associate editor coordinating the review of this manuscript and approving it for publication was Juntao Fei.

given in [20], which made the tracking error satisfy the predefined performance indexes. It should be pointed out that the better control performance can not be obtained since the effect of first-order filter error is unconsidered. Recently, the command filtered backstepping (CFB) approach was presented to deal with the “explosion of complexity” and the filter error simultaneously. By introducing the command filter and the error compensation mechanism (ECM), the “explosion of complexity” was avoided and the filter error was removed in [21]–[23]. Based on CFB technique, a new trajectory tracking control algorithm for quadrotor UAV was firstly proposed in [24]. Afterwards, several adaptive CFB control schemes have been developed in [25]–[28]. Nevertheless, these works can only achieve asymptotic convergence, and this means that the tracking error will converge to zero when the time approaches to infinity. In order to increase convergence speed of the position and attitude tracking errors, the finite-time trajectory tracking control strategy is more desirable. So far, few results on finite-time command filtered backstepping (FTCFB) adaptive trajectory tracking control schemes for quadrotor UAV have been reported, which is one motivation of this paper.

On the other hand, the position and attitude signals in the control of quadrotor UAV are generated by the computer and transmitted in communication channel, and they are required to be quantized before passing through the communication channel. Therefore, it is important to consider the quantized control for quadrotor UAV to achieve exact trajectory tracking control performance. Due to the strong coupling and nonlinear characteristics of quadrotor UAV, many significant adaptive control approaches have been proposed for nonlinear systems with quantized inputs from a theoretical perspective [29]–[31], where [29] for single-input and single-output nonlinear systems, [30] for interconnected nonlinear systems, and [31] for stochastic nonlinear systems. For quadrotor UAV with quantized input signals, in [32], a backstepping-based adaptive finite-time tracking control algorithm was presented. In [33], a composite adaptive quantized controller was constructed based on DSC technique for quadrotor UAV. Note that the control design methods in [32] and [33] are based on the backstepping and DSC technique, respectively, so the problem of “explosion of complexity” exists in [32], and the better control performance may not be obtained in [33]. Besides, although the adaptive quantized control strategies are developed [32] and [33], the prior information of quantization parameters should be required, which further limits their scope of applications.

Motivated by the abovementioned discussions, the FTCFB adaptive trajectory tracking control for quadrotor UAV with quantized inputs is investigated in this article. The designed finite-time controllers guarantee the position and attitude tracking errors converge to a small neighborhood of the origin in finite time. Compared with the existing results, the main contributions of this paper are concluded as follows.

- 1) Compared with the asymptotic convergence command filter used in [24]–[28], a novel command filter

is introduced, which can not only approximate the derivative of virtual control signal but also realize the finite-time convergence.

- 2) Unlike the existing ECM results in [24]–[28] without considering the rapid convergence, the modified fractional order ECM is designed to quickly remove the effect of filter error. Meanwhile, in contrast to the symbolic function-based ECM proposed in [34], the modified fractional order ECM are constructed by the nonsmooth signal, so the chattering phenomenon is attenuated.
- 3) Different from the quadrotor UAV with quantized inputs results in [32] and [33], the prior information of the quantization parameters for position subsystem and attitude subsystem is not required via adaptive compensation technique, which is more convenient for practical applications.

The rest of the paper is organized as follows. In Section II, the dynamic model of quadrotor UAV and some useful assumptions and lemmas are given. The finite-time adaptive control design scheme is constructed in Section III, and the stability analysis is strictly proved in Section IV. In Section V, the simulation results are illustrated to highlight the effectiveness of the proposed finite-time control algorithm. The conclusion is provided in Section VI.

II. PROBLEM FORMULATION

The simplified dynamic model of quadrotor UAV stated in [35] is given as

$$\begin{cases} \ddot{x} = \frac{\tau_F}{m} (\cos \phi \sin \theta \cos \psi + \sin \phi \sin \psi) - \frac{G_x \dot{x}}{m} + d_x \\ \ddot{y} = \frac{\tau_F}{m} (\cos \phi \sin \theta \sin \psi - \sin \phi \cos \psi) - \frac{G_y \dot{y}}{m} + d_y \\ \ddot{z} = \frac{\tau_F}{m} (\cos \phi \cos \theta) - g - \frac{G_z \dot{z}}{m} + d_z \\ \ddot{\phi} = \frac{\tau_\phi}{J_x} + \dot{\theta} \dot{\psi} \frac{J_y - J_z}{J_x} - \frac{G_\phi \dot{\phi}}{J_x} + d_\phi \\ \ddot{\theta} = \frac{\tau_\theta}{J_y} + \dot{\phi} \dot{\psi} \frac{J_x - J_z}{J_y} - \frac{G_\theta \dot{\theta}}{J_y} + d_\theta \\ \ddot{\psi} = \frac{\tau_\psi}{J_z} + \dot{\phi} \dot{\theta} \frac{J_x - J_y}{J_z} - \frac{G_\psi \dot{\psi}}{J_z} + d_\psi \end{cases}$$

where ϕ, θ, ψ are roll angle, pitch angle and yaw angle; x, y, z represent positions. m is the weight of quadrotor UAV; ℓ is the distance from the center of mass of the body to the propeller shaft; g is the acceleration of gravity. J_x, J_y, J_z are the moments of inertia of quadrotor UAV. For $i = x, y, z, \phi, \theta, \psi$, G_i is the air drag coefficients of the model, and d_i is the external disturbance. $\tau_F, \tau_\phi, \tau_\theta, \tau_\psi$ are control inputs of quadrotor UAV.

For the sake of controller design, the abovementioned model with quantized inputs is divided into the attitude subsystem and position subsystem, which are described as follows

$$\ddot{\Xi}_i = g_i q(\tau_i) + f_i + d_i, \quad i = 1, 2, 3 \quad (1)$$

$$\ddot{\Xi}_i = q(\tau_i) + f_i + d_i, \quad i = 4, 5, 6 \quad (2)$$

where $(\Xi_1, \Xi_2, \Xi_3, \Xi_4, \Xi_5, \Xi_6) = (\phi, \theta, \psi, x, y, z), (g_1, g_2, g_3) = (\frac{\ell}{J_x}, \frac{\ell}{J_y}, \frac{\ell}{J_z}), (\tau_1, \tau_2, \tau_3) = (\tau_\phi, \tau_\theta, \tau_\psi), (\tau_4, \tau_5, \tau_6) = (\frac{\tau_F}{m}(\cos \phi \sin \theta \cos \psi + \sin \phi \sin \psi), \frac{\tau_F}{m}(\cos \phi \sin \theta \sin \psi - \sin \phi \cos \psi), \frac{\tau_F}{m}(\cos \phi \cos \theta)), (f_1, f_2, f_3) = (\dot{\theta} \dot{\psi} \frac{J_y - J_z}{J_x} - \frac{G_\phi \ell}{J_x} \dot{\phi}, \dot{\phi} \dot{\psi} \frac{J_x - J_z}{J_y} - \frac{G_\theta \ell}{J_y} \dot{\theta}, \dot{\phi} \dot{\theta} \frac{J_x - J_y}{J_z} - \frac{G_\psi \ell}{J_z} \dot{\psi}), (f_4, f_5, f_6) = (-\frac{G_x \dot{x}}{m}, -\frac{G_y \dot{y}}{m}, -g - \frac{G_z \dot{z}}{m})$.

The input $q(\tau_i)$ takes the quantized values, and the following hysteretic quantizer [29] is adopted

$$q(\tau_i) = \begin{cases} \tau_m \text{sgn}(\tau_i), & \frac{\tau_m}{1 + \delta_i} < |\tau_i| \leq \tau_m, \dot{\tau}_i < 0, \text{ or} \\ & \tau_m < |\tau_i| \leq \frac{\tau_m}{1 - \delta_i}, \dot{\tau}_i > 0 \\ \tau_i(1 + \delta_i)\text{sgn}(\tau_i), & \tau_m < |\tau_i| \leq \frac{\tau_m}{1 - \delta_i}, \dot{\tau}_i < 0, \text{ or} \\ & \frac{\tau_m}{1 - \delta_i} < |\tau_i| \leq \frac{\tau_m(1 + \delta_i)}{1 - \delta_i}, \\ & \dot{\tau}_i > 0, \\ 0, & 0 \leq |\tau_i| < \frac{\tau_{\min}}{1 + \delta_i}, \dot{\tau}_i < 0, \text{ or} \\ & \frac{\tau_{\min}}{1 + \delta_i} \leq |\tau_i| < \tau_{\min}, \dot{\tau}_i > 0 \\ q(\tau_i(t^-)), & \text{othercases} \end{cases}$$

where $\tau_m = \rho_i^{1-m} \tau_{\min}, m = 1, 2, \dots, \tau_{\min} > 0, 0 < \rho_i < 1$, and $\delta_i = \frac{1-\rho_i}{1+\rho_i}$; $q(\tau_i)$ is the set $U = \{0, \pm \tau_m, \pm \tau_m(1 + \delta_i)\}$. Based on the results in [31], $q(\tau_i)$ is decomposed in the following form

$$q(\tau_i) = H_i(\tau_i)\tau_i(t) + L_i(t) \quad (3)$$

where

$$H_i(\tau_i) = \begin{cases} \frac{q(\tau_i)}{\tau_i}, & |\tau_i| > \tau_{\min} \\ 1, & |\tau_i| \leq \tau_{\min} \end{cases}$$

$$L_i(t) = \begin{cases} 0, & |\tau_i| > \tau_{\min} \\ -\tau_i, & |\tau_i| \leq \tau_{\min} \end{cases}$$

and $H_i(\tau_i)$ and $L_i(t)$ satisfy

$$1 - \delta_i \leq H_i(\tau_i) \leq 1 + \delta_i, \quad |L_i(t)| \leq \tau_{\min}. \quad (4)$$

The main control objective of this paper is to design a FTCFB adaptive quantized control scheme for quadrotor UAV, which enables the output of quadrotor UAV faster track the desired reference trajectories $y_{d,x}, y_{d,y}, y_{d,z}, y_{d,\psi}$, and the finite-time boundedness of all signals in the closed-loop system is guaranteed.

Assumption 1: For $i = x, y, z, \psi$, the desired trajectories $y_{d,i}$ and its first derivative $\dot{y}_{d,i}$ are known and bounded.

Assumption 2: The external disturbance d_i is bounded, and it satisfies $|d_i| \leq d_{i,\max}$.

Lemma 1 ([34]): For a nonlinear system $\dot{x} = f(x)$, there exist a continuous positive definite function $F(x)$ and scalars $\mu_1 > 0, \mu_2 > 0, 0 < \varsigma < 1, 0 < \iota < \infty$ such that $\dot{F}(x) \leq -\mu_1 F(x) - \mu_2 F(x)^\varsigma + \iota$, then the solution of $\dot{x} = f(x)$ is practical finite-time stable, where the setting time T_r is bounded

by $T_r \leq \max\{t_0 + \frac{1}{\varpi_0 \mu_1(1-\varsigma)} \ln \frac{\varpi_0 \mu_1 F^{1-\varsigma}(t_0) + \mu_2}{\mu_2}, t_0 + \frac{1}{\mu_1(1-\varsigma)} \ln \frac{\eta_1 F^{1-\varsigma}(t_0) + \varpi_0 \mu_2}{\varpi_0 \mu_2}\}$, and ϖ_0 satisfies $0 < \varpi_0 < 1$.

Lemma 2 ([36]): Assume that $F(X)$ is a continuous function defined on a compact set Ω . For any given constant $\varepsilon > 0$, there exists a fuzzy logical system $W^\top S(X)$ such that

$$\sup_{X \in \Omega} |F(X) - W^\top S(X)| \leq \varepsilon$$

where $W = [W_1, \dots, W_N]^\top \in \mathbb{R}^N$ is the weight vector; $S(X) = [S_1(X), S_2(X), \dots, S_N(X)]^\top / \sum_{i=1}^N S_i(X) \in \mathbb{R}^N$, and $S_i(X)$ is the commonly Gaussian function defined by $S_i(X) = \exp\left[-\frac{(X-\mu_i)^\top(X-\mu_i)}{\eta_i^2}\right]$ with $\mu_i = [\mu_{i,1}, \mu_{i,2}, \dots, \mu_{i,n}]^\top$ and η_i being the center vector and the width of the Gaussian function, respectively.

Lemma 3 ([37]): Suppose that $\alpha > 0, \beta > 0$, and $\lambda(p, q) > 0$ is a real valued function, the following inequality holds

$$|p|^\alpha |q|^\beta \leq \frac{\alpha \lambda(p, q) |p|^{\alpha+\beta}}{\alpha + \beta} + \frac{\beta \lambda(p, q)^{-\frac{\alpha}{\beta}} |q|^{\alpha+\beta}}{\alpha + \beta}.$$

Lemma 4 ([38]): For $\xi_i \in \mathbb{R}, i = 1, \dots, M$, and $0 < \nu \leq 1$, one has

$$\left(\sum_{i=1}^M |\xi_i|\right)^\nu \leq \sum_{i=1}^M |\xi_i|^\nu \leq M^{1-\nu} \left(\sum_{i=1}^M |\xi_i|\right)^\nu.$$

III. POSITION AND ATTITUDE CONTROLLERS DESIGN

In this section, a novel finite-time adaptive trajectory tracking control scheme for quadrotor UAV is proposed via FTCFB method, where the position controller and attitude controller are designed, respectively.

Firstly, the tracking errors are constructed as follows

$$\chi_{i,1} = \Xi_i - y_{d,i} \quad (5)$$

$$\chi_{i,2} = \hat{\Xi}_i - \bar{\Lambda}_{i,1} \quad (6)$$

where $y_{d,i}$ is the corresponding desired trajectory; $\bar{\Lambda}_{i,1}$ is the output of finite-time command filter with the virtual control signal $\Lambda_{i,1}$ as filter input signal. The finite-time command filter borrowed from [39] is given as

$$\begin{cases} \dot{\phi}_{i,1} = \phi_{i,2} \\ \dot{\phi}_{i,2} = \frac{1}{\epsilon_i^2} \left(-a_{i,1} \arctan(\phi_{i,1} - \Lambda_{i,1}) \right. \\ \left. - a_{i,2} \arctan(\epsilon_i \phi_{i,2}) \right) \end{cases} \quad (7)$$

where $\epsilon_i, a_{i,1}$ and $a_{i,2}$ are positive constants, $\bar{\Lambda}_{i,1} = \phi_{i,1}$ $\bar{\Lambda}_{i,1} = \phi_{i,2}$. There exist constants $\tau > 0, \rho > 0$ such that

$$\phi_{i,1} - \Lambda_{i,1} = \mathcal{O}_i(\epsilon_i^{\rho\tau}) \quad (8)$$

where $\mathcal{O}_i(\epsilon_i^{\rho\tau})$ denotes the degree of approximation between $\phi_{i,1}$ and $\Lambda_{i,1}$.

Remark 1: Note that the command filters in [24]–[28] can merely ensure the asymptotic convergence, so the output signal of command filter can not faster approximate the

derivative of virtual control signal. Although the command filter in [34] has the characteristic of finite-time convergence, the chattering phenomenon may arise. For the command filter in (7), the finite-time convergence is achieved and the chattering phenomenon is also attenuated at the same time.

Furthermore, define the compensated tracking errors

$$v_{i,1} = \chi_{i,1} - \kappa_{i,1} \quad (9)$$

$$v_{i,2} = \chi_{i,2} - \kappa_{i,2} \quad (10)$$

where the compensated signal $\kappa_{i,1}$ and $\kappa_{i,2}$ will be given later.

A. CONTROLLER DESIGN FOR ATTITUDE SUBSYSTEM

Step *i*, 1: According to the error transformations (5), (6) and (9), the time derivative of $v_{i,1}$ ($i = 1, 2, 3$) is given as

$$\dot{v}_{i,1} = \chi_{i,2} + (\bar{\Lambda}_{i,1} - \Lambda_{i,1}) + \Lambda_{i,1} - \dot{y}_{d,i} - \dot{\kappa}_{i,1}. \quad (11)$$

The virtual control signal $\Lambda_{i,1}$ is designed as

$$\Lambda_{i,1} = -c_{i,1}\chi_{i,1} + \dot{y}_{d,i} - s_{i,1}v_{i,1}^\gamma \quad (12)$$

where $c_{i,1}, s_{i,1}$ are positive design parameters; $1/2 < \gamma = \gamma_1/\gamma_2 < 1$, γ_1, γ_2 are positive odd integers. The compensated signal $\kappa_{i,1}$ is chosen as

$$\dot{\kappa}_{i,1} = -c_{i,1}\kappa_{i,1} + \kappa_{i,2} + (\bar{\Lambda}_{i,1} - \Lambda_{i,1}) - h_{i,1}\kappa_{i,1}^\gamma \quad (13)$$

where $h_{i,1} > 0$ is a design constant, and the initial condition is $\kappa_{i,1}(0) = 0$.

Choose the Lyapunov function candidate $V_{i,1} = \frac{1}{2}v_{i,1}^2 + \frac{1}{2}\kappa_{i,1}^2$. Based on (11) and (13), the time derivative of $V_{i,1}$ is calculated as

$$\begin{aligned} \dot{V}_{i,1} = & -c_{i,1}v_{i,1}^2 - s_{i,1}v_{i,1}^{1+\gamma} + v_{i,1}v_{i,2} + h_{i,1}v_{i,1}\kappa_{i,1}^\gamma \\ & - c_{i,1}\kappa_{i,1}^2 - h_{i,1}\kappa_{i,1}^{1+\gamma} + \kappa_{i,1}(\bar{\Lambda}_{i,1} - \Lambda_{i,1}) \\ & + \kappa_{i,1}\kappa_{i,2}. \end{aligned} \quad (14)$$

Step *i*, 2: In light of (1), (6) and (10), the time derivative of $v_{i,2}$ is obtained

$$\dot{v}_{i,2} = g_i H_i(\tau_i)\tau_i + g_i L_i + f_i + d_i - \dot{\bar{\Lambda}}_{i,1} - \dot{\kappa}_{i,2}. \quad (15)$$

Given that f_i is an unknown nonlinear function, so the designed controller cannot contain f_i due to the realizability. From Lemma 2, for any given constant $\varepsilon_i > 0$, a fuzzy logical system $W_i^\top S_i(\bar{\Xi})$ is applied to identify the function f_i such that $f_i = W_i^\top S_i(\bar{\Xi}) + \Delta_i(\bar{\Xi})$, $|\Delta_i(\bar{\Xi})| \leq \varepsilon_i$, $\bar{\Xi} = [\bar{\Xi}_1, \bar{\Xi}_2, \bar{\Xi}_3]$. By using Young's inequality, one has

$$\begin{aligned} v_{i,2}f_i = & v_{i,2}W_i^\top S_i + v_{i,2}\Delta_i \\ \leq & \frac{v_{i,2}^2 \|W_i\|^2 S_i^\top S_i}{2l_i^2} + \frac{1}{2}l_i^2 + \frac{1}{2}v_{i,2}^2 + \frac{1}{2}\varepsilon_i^2 \end{aligned} \quad (16)$$

where $l_i > 0$ is a design parameter. Define unknown constants $\Theta_i = \{\|W_i\|^2\}$, $i = 1, 2, 3$, and $\tilde{\Theta}_i = \Theta_i - \hat{\Theta}_i$ is the estimate error.

The compensated signal $\kappa_{i,2}$ is chosen as

$$\dot{\kappa}_{i,2} = -c_{i,2}\kappa_{i,2} - \kappa_{i,1} - h_{i,2}\kappa_{i,2}^\gamma \quad (17)$$

with $c_{i,2}$ and $h_{i,2}$ being positive design parameters. Define $b_i = g_i(1 - \delta_i)$, $p_i = \frac{1}{b_i}$, $i = 1, 2, 3$, and $\tilde{p}_i = p_i - \hat{p}_i$ is the estimate error. The actual controller τ_i is designed as

$$\begin{cases} \Lambda_{i,2} = c_{i,2}\chi_{i,2} + \chi_{i,1} + s_{i,2}v_{i,2}^\gamma - \dot{\bar{\Lambda}}_{i,1} \\ \quad + \frac{v_{i,2}\hat{\Theta}_i S_i^\top S_i}{2l_i^2} + \frac{3}{2}v_{i,2} \\ \tau_i = -\frac{v_{i,2}\hat{p}_i^2 \Lambda_{i,2}^2}{\sqrt{v_{i,2}^2 \hat{p}_i^2 \Lambda_{i,2}^2 + \omega_i^2}} \end{cases} \quad (18)$$

where $s_{i,2}, \omega_i$ are positive design parameters. The parameter update laws $\hat{\Theta}_i$ and \hat{p}_i are constructed as follows

$$\dot{\hat{\Theta}}_i = \frac{m_i v_{i,2}^2 S_i^\top S_i}{2l_i^2} - \sigma_i \hat{\Theta}_i \quad (19)$$

$$\dot{\hat{p}}_i = n_i v_{i,2} \Lambda_{i,2} - r_i \hat{p}_i \quad (20)$$

where m_i, n_i, r_i and σ_i are positive constants.

Consider the following Lyapunov function $V_i = V_{i,1} + \frac{1}{2}v_{i,2}^2 + \frac{1}{2}\kappa_{i,2}^2 + \frac{1}{2m_i}\tilde{\Theta}_i^2 + \frac{b_i}{2n_i}\tilde{p}_i^2$. The time derivative of V_i is computed as

$$\begin{aligned} \dot{V}_i = & \dot{V}_{i,1} + v_{i,2}(g_i H_i \tau_i + g_i L_i + f_i + d_i - \dot{\bar{\Lambda}}_{i,1} - \dot{\kappa}_{i,2}) \\ & + \kappa_{i,2}\dot{\kappa}_{i,2} - \frac{1}{m_i}\tilde{\Theta}_i\dot{\hat{\Theta}}_i - \frac{b_i}{n_i}\tilde{p}_i\dot{\hat{p}}_i. \end{aligned} \quad (21)$$

From Assumption 2, equation (4) and Young's inequality, the following inequalities hold

$$v_{i,2}d_i \leq \frac{1}{2}v_{i,2}^2 + \frac{1}{2}d_{i,\max}^2 \quad (22)$$

$$v_{i,2}g_i L_i \leq \frac{1}{2}v_{i,2}^2 + \frac{1}{2}g_i^2 \tau_{\min}^2. \quad (23)$$

According to the fact $0 \leq |\varepsilon| - \frac{\varepsilon^2}{\sqrt{\varepsilon^2 + \eta^2}} < \eta$, one yields

$$\begin{aligned} v_{i,2}g_i H_i u_i = & -g_i H_i \frac{v_{i,2}^2 \hat{p}_i^2 \Lambda_{i,2}^2}{\sqrt{v_{i,2}^2 \hat{p}_i^2 \Lambda_{i,2}^2 + \omega_i^2}} \\ \leq & -b_i \frac{v_{i,2}^2 \hat{p}_i^2 \Lambda_{i,2}^2}{\sqrt{v_{i,2}^2 \hat{p}_i^2 \Lambda_{i,2}^2 + \omega_i^2}} \\ \leq & b_i (\omega_i - \hat{p}_i |v_{i,2} \Lambda_{i,2}|). \end{aligned} \quad (24)$$

Thus, it follows that

$$\begin{aligned} v_{i,2}g_i H_i \tau_i + v_{i,2}\Lambda_{i,2} - \frac{b_i}{n_i}\tilde{p}_i\dot{\hat{p}}_i \\ \leq b_i (\omega_i - \hat{p}_i |v_{i,2} \Lambda_{i,2}|) + v_{i,2}\Lambda_{i,2} - b_i \tilde{p}_i v_{i,2} \Lambda_{i,2} + \frac{r_i b_i}{n_i} \tilde{p}_i \hat{p}_i \\ = b_i \omega_i + \frac{r_i b_i}{n_i} \tilde{p}_i \hat{p}_i. \end{aligned} \quad (25)$$

By substituting (16)–(20) and (22), (23), (25) into (21), one has

$$\begin{aligned} \dot{V}_i \leq & -\sum_{j=1}^2 \left(c_{i,j} v_{i,j}^2 + s_{i,j} v_{i,j}^{1+\gamma} + c_{i,j} \kappa_{i,j}^2 + h_{i,j} \kappa_{i,j}^{1+\gamma} \right. \\ & \left. - h_{i,j} v_{i,j} \kappa_{i,j}^\gamma \right) + \kappa_{i,1} (\bar{\Lambda}_{i,1} - \Lambda_{i,1}) \end{aligned}$$

$$\begin{aligned}
 & + \frac{\sigma_i}{m_i} \tilde{\Theta}_i \hat{\Theta}_i + \frac{r_i b_i}{n_i} \tilde{p}_i \hat{p}_i + b_i \omega_i + \frac{1}{2} g_i^2 \tau_{\min}^2 \\
 & + \frac{1}{2} d_{i,\max}^2 + \frac{1}{2} l_i^2 + \frac{1}{2} \varepsilon_i^2. \quad (26)
 \end{aligned}$$

Based on $|\bar{\Lambda}_{i,1} - \Lambda_{i,1}| = \mathcal{O}_i(\varepsilon_i^{2\rho\tau})$ and Young's inequality, the following inequality can be obtained

$$\kappa_{i,1} (\bar{\Lambda}_{i,1} - \Lambda_{i,1}) \leq \frac{1}{2} \kappa_{i,1}^2 + \frac{1}{2} \mathcal{O}_i(\varepsilon_i^{2\rho\tau}). \quad (27)$$

By applying Lemma 3 to the term $h_{i,j} v_{i,j} \kappa_{i,j}^\gamma$, one has

$$h_{i,j} v_{i,j} \kappa_{i,j}^\gamma \leq \frac{h_{i,j}}{1+\gamma} |v_{i,j}|^{1+\gamma} + \frac{\gamma h_{i,j}}{1+\gamma} |\kappa_{i,j}|^{1+\gamma}. \quad (28)$$

Substituting (27)–(28) into (26) results in

$$\begin{aligned}
 \dot{V}_i \leq & - \sum_{j=1}^2 c_{i,j} v_{i,j}^2 - \sum_{j=1}^2 \left(s_{i,j} - \frac{h_{i,j}}{1+\gamma} \right) v_{i,j}^{1+\gamma} \\
 & - \left(c_{i,1} - \frac{1}{2} \right) \kappa_{i,1}^2 - c_{i,2} \kappa_{i,2}^2 - \sum_{j=1}^2 \frac{h_{i,j}}{1+\gamma} \kappa_{i,j}^{1+\gamma} \\
 & - \frac{\sigma_i}{2m_i} \tilde{\Theta}_i^2 - \frac{r_i b_i}{2n_i} \tilde{p}_i^2 + \frac{\sigma_i}{2m_i} \Theta_i^2 + \frac{r_i b_i}{2n_i} p_i^2 \\
 & + \frac{1}{2} \left(\mathcal{O}_i(\varepsilon_i^{2\rho\tau}) + g_i^2 \tau_{\min}^2 + d_{i,\max}^2 + l_i^2 + \varepsilon_i^2 \right) \\
 & + b_i \omega_i. \quad (29)
 \end{aligned}$$

B. CONTROLLER DESIGN FOR POSITION SUBSYSTEM

Step *i*, 1: On the basis of (5), (6) and (9), taking the time derivative of $v_{i,1}$ ($i = 4, 5, 6$) yields

$$\dot{v}_{i,1} = \chi_{i,2} + (\bar{\Lambda}_{i,1} - \Lambda_{i,1}) + \Lambda_{i,1} - \dot{y}_{d,i} - \dot{\kappa}_{i,1}. \quad (30)$$

The virtual control signal $\Lambda_{i,1}$ and compensated signal $\kappa_{i,1}$ are given as

$$\Lambda_{i,1} = -c_{i,1} \chi_{i,1} + \dot{y}_{d,i} - s_{i,1} v_{i,1}^\gamma \quad (31)$$

$$\dot{\kappa}_{i,1} = -c_{i,1} \kappa_{i,1} + \kappa_{i,2} + (\bar{\Lambda}_{i,1} - \Lambda_{i,1}) - h_{i,1} \kappa_{i,1}^\gamma \quad (32)$$

where $c_{i,1}$, $s_{i,1}$ and $h_{i,1}$ are positive constants; $1/2 < \gamma = \gamma_1/\gamma_2 < 1$, γ_1, γ_2 are positive odd integers, and the initial condition of $\kappa_{i,1}$ is set as $\kappa_{i,1}(0) = 0$.

Choose the Lyapunov function candidate as $V_{i,1} = \frac{1}{2} v_{i,1}^2 + \frac{1}{2} \kappa_{i,1}^2$, and the time derivative of $V_{i,1}$ is computed as

$$\begin{aligned}
 \dot{V}_{i,1} = & -c_{i,1} v_{i,1}^2 - s_{i,1} v_{i,1}^{1+\gamma} + v_{i,1} v_{i,2} + h_{i,1} v_{i,1} \kappa_{i,1}^\gamma \\
 & - c_{i,1} \kappa_{i,1}^2 - h_{i,1} \kappa_{i,1}^{1+\gamma} + \kappa_{i,1} (\bar{\Lambda}_{i,1} - \Lambda_{i,1}) \\
 & + \kappa_{i,1} \kappa_{i,2}. \quad (33)
 \end{aligned}$$

Step *i*, 2: From (2), (6) and (10), the time derivative of $v_{i,2}$ can be alternated as

$$\dot{v}_{i,2} = H_i(\tau_i) \tau_i + L_i + f_i + d_i - \dot{\bar{\Lambda}}_{i,1} - \dot{\kappa}_{i,2}. \quad (34)$$

Consider the estimate errors $\tilde{\Theta}_i = \Theta_i - \hat{\Theta}_i$, where unknown constants are defined as $\Theta_i = \{\|W_i\|^2\}$, $i = 4, 5, 6$. Similar to (16), the following inequality can be obtained

$$v_{i,2} f_i = v_{i,2} W_i^\top S_i + v_{i,2} \Delta_i$$

$$\leq \frac{v_{i,2}^2 \|W_i\|^2 S_i^\top S_i}{2l_i^2} + \frac{1}{2} l_i^2 + \frac{1}{2} v_{i,2}^2 + \frac{1}{2} \varepsilon_i^2 \quad (35)$$

with $l_i > 0$ being a design constant.

The compensated signal $\kappa_{i,2}$ is designed as

$$\dot{\kappa}_{i,2} = -c_{i,2} \kappa_{i,2} - \kappa_{i,1} - h_{i,2} \kappa_{i,2}^\gamma \quad (36)$$

where $c_{i,2} > 0$, $h_{i,2} > 0$. For $i = 4, 5, 6$, define $b_i = 1 - \delta_i$, $p_i = \frac{1}{b_i}$, and $\tilde{p}_i = p_i - \hat{p}_i$. Construct the actual controller τ_i as follows

$$\begin{cases} \Lambda_{i,2} = c_{i,2} \chi_{i,2} + \chi_{i,1} + s_{i,2} v_{i,2}^\gamma - \dot{\bar{\Lambda}}_{i,1} \\ \quad + \frac{v_{i,2} \hat{\Theta}_i S_i^\top S_i}{2l_i^2} + \frac{3}{2} v_{i,2} \\ \tau_i = -\frac{v_{i,2} \hat{p}_i^2 \Lambda_{i,2}}{\sqrt{v_{i,2}^2 \hat{p}_i^2 \Lambda_{i,2}^2 + \omega_i^2}} \end{cases} \quad (37)$$

where $s_{i,2} > 0$, $\omega_i > 0$ are design parameters. The parameter update laws $\hat{\Theta}_i$ and \hat{p}_i are selected as

$$\dot{\hat{\Theta}}_i = \frac{m_i v_{i,2}^2 S_i^\top S_i}{2l_i^2} - \sigma_i \hat{\Theta}_i \quad (38)$$

$$\dot{\hat{p}}_i = n_i v_{i,2} \Lambda_{i,2} - r_i \hat{p}_i \quad (39)$$

where m_i, n_i, r_i and σ_i are positive constants.

Consider the following Lyapunov function $V_i = V_{i,1} + \frac{1}{2} v_{i,2}^2 + \frac{1}{2} \kappa_{i,2}^2 + \frac{1}{2m_i} \tilde{\Theta}_i^2 + \frac{b_i}{2n_i} \tilde{p}_i^2$. The time derivative of V_i is calculated as

$$\begin{aligned}
 \dot{V}_i = & \dot{V}_{i,1} + v_{i,2} \left(H_i \tau_i + L_i + f_i + d_i - \dot{\bar{\Lambda}}_{i,1} - \dot{\kappa}_{i,2} \right) \\
 & + \kappa_{i,2} \dot{\kappa}_{i,2} - \frac{1}{m_i} \tilde{\Theta}_i \dot{\tilde{\Theta}}_i - \frac{b_i}{n_i} \tilde{p}_i \dot{\tilde{p}}_i. \quad (40)
 \end{aligned}$$

Obviously, the following inequalities hold

$$v_{i,2} d_i \leq \frac{1}{2} v_{i,2}^2 + \frac{1}{2} d_{i,\max}^2 \quad (41)$$

$$v_{i,2} L_i \leq \frac{1}{2} v_{i,2}^2 + \frac{1}{2} \tau_{\min}^2. \quad (42)$$

According to (37) and based on the fact that $0 \leq |\varepsilon| - \frac{\varepsilon^2}{\sqrt{\varepsilon^2 + \eta^2}} < \eta$, one gets

$$\begin{aligned}
 v_{i,2} H_i \tau_i = & -H_i \frac{v_{i,2}^2 \hat{p}_i^2 \Lambda_{i,2}^2}{\sqrt{v_{i,2}^2 \hat{p}_i^2 \Lambda_{i,2}^2 + \omega_i^2}} \\
 \leq & -b_i \frac{v_{i,2}^2 \hat{p}_i^2 \Lambda_{i,2}^2}{\sqrt{v_{i,2}^2 \hat{p}_i^2 \Lambda_{i,2}^2 + \omega_i^2}} \\
 \leq & b_i (\omega_i - \hat{p}_i |v_{i,2} \Lambda_{i,2}|). \quad (43)
 \end{aligned}$$

Furthermore, one has

$$\begin{aligned}
 v_{i,2} H_i u_i + v_{i,2} \Lambda_{i,2} - \frac{r_i}{n_i} \tilde{p}_i \dot{\tilde{p}}_i \\
 \leq b_i (\omega_i - \hat{p}_i |v_{i,2} \Lambda_{i,2}|) + v_{i,2} \Lambda_{i,2} - b_i \tilde{p}_i v_{i,2} \Lambda_{i,2} + \frac{r_i b_i}{n_i} \tilde{p}_i \hat{p}_i \\
 = b_i \omega_i + \frac{r_i b_i}{n_i} \tilde{p}_i \hat{p}_i. \quad (44)
 \end{aligned}$$

Similarly to the processing method (26)–(28) in subsection III-A, it is easily verified that

$$\begin{aligned} \dot{V}_i \leq & -\sum_{j=1}^2 c_{i,j} v_{i,j}^2 - \sum_{j=1}^2 \left(s_{i,j} - \frac{h_{i,j}}{1+\gamma} \right) v_{i,j}^{1+\gamma} \\ & - \left(c_{i,1} - \frac{1}{2} \right) \kappa_{i,1}^2 - c_{i,2} \kappa_{i,2}^2 - \sum_{j=1}^2 \frac{h_{i,j}}{1+\gamma} \kappa_{i,j}^{1+\gamma} \\ & - \frac{\sigma_i}{2m_i} \tilde{\Theta}_i^2 - \frac{r_i b_i}{2n_i} \tilde{p}_i^2 + \frac{\sigma_i}{2m_i} \Theta_i^2 + \frac{r_i b_i}{2n_i} p_i^2 + b_i \omega_i \\ & + \frac{1}{2} \left(\mathcal{O}_i \left(\epsilon_i^{2\rho\tau} \right) + \tau_{\min}^2 + d_{i,\max}^2 + l_i^2 + \varepsilon_i^2 \right). \end{aligned} \quad (45)$$

In the design of double closed-loop controller, the desired signals of roll angle and pitch angle can be obtained by the control input of position subsystem and the reference trajectory of given yaw angle

$$\tau_6 = \frac{\tau_F}{m} (\cos \phi \cos \theta) \quad (46)$$

$$\tau_4 = \frac{\tau_F}{m} (\cos \phi \sin \theta \cos \psi + \sin \phi \sin \psi) \quad (47)$$

$$\tau_5 = \frac{\tau_F}{m} (\cos \phi \sin \theta \sin \psi - \sin \phi \cos \psi). \quad (48)$$

Based on (46)–(48), the desired roll angle and pitch angle are given as

$$\theta_d = \arctan \left(\frac{\tau_4 \cos \psi + \tau_5 \sin \psi}{\tau_6} \right) \quad (49)$$

$$\phi_d = \arctan \left(\frac{\tau_4 \sin \psi - \tau_5 \cos \psi}{\tau_6} \cos \theta_d \right) \quad (50)$$

and the total lift force is calculated as

$$\tau_F = \frac{m \tau_6}{\cos \phi_d \cos \theta_d}. \quad (51)$$

Remark 2: In previous works [24]–[28], the traditional ECM is designed to remove the effect of filter error. However, it is difficult to ensure faster convergence rate. In our results, the modified fractional order ECM is designed to fleetly eliminate the effect of filter error. In particular, when the design constant $h_{i,k}$ is set as $h_{i,k} = 0$, the modified fractional order ECM reduces to the traditional ECM. Therefore, the proposed modified fractional order ECM contains the traditional ECM as a special case, which is more effective.

IV. STABILITY ANALYSIS

Theorem 1: For the quadrotor UAV with quantized inputs when the Assumptions 1–2 satisfied, the actual controllers (18), (37) with the virtual control signals (12), (31) and the parameter update laws (19), (20), (38), (39) together with finite-time command filter (7) guarantee that all signals in closed-loop system are bounded in finite-time, and the tracking errors will converge to a sufficiently small neighborhood of the origin in finite time by tuning properly design parameters.

Proof: Choose the Lyapunov function $V = \sum_{i=1}^6 V_i$. In light of (29) and (45), the time derivative of V is given as

$$\begin{aligned} \dot{V} \leq & \sum_{i=1}^6 \left\{ -\sum_{j=1}^2 c_{i,j} v_{i,j}^2 - \sum_{j=1}^2 \left(s_{i,j} - \frac{h_{i,j}}{1+\gamma} \right) v_{i,j}^{1+\gamma} \right. \\ & - \left(c_{i,1} - \frac{1}{2} \right) \kappa_{i,1}^2 - c_{i,2} \kappa_{i,2}^2 - \sum_{j=1}^2 \frac{h_{i,j}}{1+\gamma} \kappa_{i,j}^{1+\gamma} \\ & - \frac{\sigma_i}{2m_i} \tilde{\Theta}_i^2 - \frac{r_i b_i}{2n_i} \tilde{p}_i^2 - k_i \left(\frac{\tilde{\Theta}_i^2}{2m_i} \right)^{\frac{1+\gamma}{2}} + k_i \left(\frac{\tilde{\Theta}_i^2}{2m_i} \right)^{\frac{1+\gamma}{2}} \\ & - \lambda_i \left(\frac{b_i \tilde{p}_i^2}{2n_i} \right)^{\frac{1+\gamma}{2}} + \lambda_i \left(\frac{b_i \tilde{p}_i^2}{2n_i} \right)^{\frac{1+\gamma}{2}} + \frac{\sigma_i \Theta_i^2}{2m_i} + b_i \omega_i \\ & \left. + \frac{r_i b_i}{2n_i} p_i^2 + \frac{1}{2} \left(\mathcal{O}_i \left(\epsilon_i^{2\rho\tau} \right) + d_{i,\max}^2 + l_i^2 + \varepsilon_i^2 \right) \right\} \\ & + \frac{1}{2} \sum_{i=1}^3 (g_i^2 + 1) \tau_{\min}^2 \end{aligned} \quad (52)$$

where k_i and λ_i are positive constants.

By applying Lemma 3 to the terms $\left(\frac{\tilde{\Theta}_i^2}{2m_i} \right)^{\frac{1+\gamma}{2}}$ and $\left(\frac{b_i \tilde{p}_i^2}{2n_i} \right)^{\frac{1+\gamma}{2}}$, there exists a constant ϑ satisfied $0 < \vartheta < 1$ such that

$$\left(\frac{\tilde{\Theta}_i^2}{2m_i} \right)^{\frac{1+\gamma}{2}} \leq \frac{\vartheta}{2m_i} \tilde{\Theta}_i^2 + \frac{(1-\gamma)}{2} \left(\frac{\vartheta^{-1}(1+\gamma)}{2} \right)^{\frac{1+\gamma}{1-\gamma}} \quad (53)$$

$$\left(\frac{b_i \tilde{p}_i^2}{2n_i} \right)^{\frac{1+\gamma}{2}} \leq \frac{\vartheta b_i}{2n_i} \tilde{p}_i^2 + \frac{(1-\gamma)}{2} \left(\frac{\vartheta^{-1}(1+\gamma)}{2} \right)^{\frac{1+\gamma}{1-\gamma}}. \quad (54)$$

Thus, the inequality (52) can be rewritten as

$$\begin{aligned} \dot{V} \leq & \sum_{i=1}^6 \left\{ -\sum_{j=1}^2 c_{i,j} v_{i,j}^2 - \sum_{j=1}^2 \left(s_{i,j} - \frac{h_{i,j}}{1+\gamma} \right) v_{i,j}^{1+\gamma} \right. \\ & - \left(c_{i,1} - \frac{1}{2} \right) \kappa_{i,1}^2 - c_{i,2} \kappa_{i,2}^2 - \sum_{j=1}^2 \frac{h_{i,j}}{1+\gamma} \kappa_{i,j}^{1+\gamma} \\ & - (\sigma_i - k_i \vartheta) \frac{\tilde{\Theta}_i^2}{2m_i} - (r_i - \lambda_i \vartheta) \frac{b_i \tilde{p}_i^2}{2n_i} \\ & - k_i \left(\frac{\tilde{\Theta}_i^2}{2m_i} \right)^{\frac{1+\gamma}{2}} - \lambda_i \left(\frac{b_i \tilde{p}_i^2}{2n_i} \right)^{\frac{1+\gamma}{2}} + \frac{\sigma_i \Theta_i^2}{2m_i} \\ & \left. + \frac{r_i b_i}{2n_i} p_i^2 + (k_i + \lambda_i) \frac{(1-\gamma)}{2} \left(\frac{\vartheta^{-1}(1+\gamma)}{2} \right)^{\frac{1+\gamma}{1-\gamma}} \right. \\ & \left. + \frac{1}{2} \left(\mathcal{O}_i \left(\epsilon_i^{2\rho\tau} \right) + d_{i,\max}^2 + l_i^2 + \varepsilon_i^2 \right) + b_i \omega_i \right\} \\ & + \frac{1}{2} \sum_{i=1}^3 (g_i^2 + 1) \tau_{\min}^2 \\ \leq & -\mu_1 V - \mu_2 V^{\frac{1+\gamma}{2}} + \iota \end{aligned} \quad (55)$$

where $\mu_1 = \min\{2c_{i,j}, 2(c_{i,1} - \frac{1}{2}), \sigma_i - k_i\vartheta, r_i - \lambda_i\vartheta\}$, $\mu_2 = \min\{2^{\frac{1+\gamma}{2}}(s_{i,j} - \frac{h_{i,j}}{1+\gamma}), 2^{\frac{1+\gamma}{2}}\frac{h_{i,j}}{1+\gamma}, k_i, \lambda_i\}$, $\iota = \sum_{i=1}^6(\frac{\sigma_i\vartheta_i^2}{2m_i} + \frac{r_i b_i}{2n_i} p_i^2 + (k_i + \lambda_i)\frac{(1-\gamma)}{2}(\frac{\vartheta^{-1}(1+\gamma)}{2})^{\frac{1+\gamma}{1-\gamma}} + b_i\omega_i + \frac{1}{2}(\mathcal{O}_i(\epsilon_i^{2\rho\tau}) + d_{i,\max}^2 + l_i^2 + \varepsilon_i^2)) + \frac{1}{2}\sum_{i=1}^3(g_i^2 + 1)\tau_{\min}^2$.

Therefore, (55) is changed as follows

$$\dot{V} \leq -\varpi_0\mu_1 V - (1 - \varpi_0)\mu_1 V - \mu_2 V^{\frac{1+\gamma}{2}} + \iota \quad (56)$$

or

$$\dot{V} \leq -\mu_1 V - \varpi_0\mu_2 V^{\frac{1+\gamma}{2}} - (1 - \varpi_0)\mu_2 V^{\frac{1+\gamma}{2}} + \iota \quad (57)$$

where $0 < \varpi_0 < 1$. With help of (56), if $V > \iota/((1 - \varpi_0)\mu_1)$, then $\dot{V} \leq -\varpi_0\mu_1 V - \mu_2 V^{\frac{1+\gamma}{2}}$. Based on Lemma 1, $v_{i,j}, \kappa_{i,j}$ and $\tilde{\Theta}_i, \tilde{p}_i$ will converge into the following region

$$(v_{i,j}, \kappa_{i,j}, \tilde{\Theta}_i, \tilde{p}_i) \in \left\{ V \leq \frac{\iota}{(1 - \varpi_0)\mu_1} \right\} \quad (58)$$

in finite time $T_{i,1} \leq (2/(\varpi_0\mu_1(1 - \gamma))) \ln((\varpi_0\mu_1 V^{\frac{1-\gamma}{2}}(0) + \mu_2)/\mu_2)$. In light of (57), $\dot{V} \leq -\mu_1 V - \varpi_0\mu_2 V^{\frac{1+\gamma}{2}}$ is obtained when $V^{\frac{1+\gamma}{2}} > \iota/((1 - \varpi_0)\mu_2)$. In the same way, $v_{i,j}, \kappa_{i,j}$ and $\tilde{\Theta}_i, \tilde{p}_i$ are driven into the following region

$$(v_{i,j}, \kappa_{i,j}, \tilde{\Theta}_i, \tilde{p}_i) \in \left\{ V \leq \left(\frac{\iota}{(1 - \varpi_0)\mu_2} \right)^{\frac{2}{1+\gamma}} \right\} \quad (59)$$

within finite time $T_{i,2} \leq (2/(\mu_1(1 - \gamma))) \ln((\mu_1 V^{\frac{1-\gamma}{2}}(0) + \varpi_0\mu_2)/\varpi_0\mu_2)$. Thus, the finite-time boundedness of all signals $v_{i,j}, \kappa_{i,j}$ and $\tilde{\Theta}_i, \tilde{p}_i$ in closed-loop system is achieved.

It means that $v_{i,1}$ and $\kappa_{i,1}$ will converge into the region

$$|v_{i,1}| \leq \min \left\{ \sqrt{\frac{2\iota}{(1 - \varpi_0)\mu_1}}, \sqrt{2 \left(\frac{\iota}{(1 - \varpi_0)\mu_2} \right)^{\frac{2}{1+\gamma}}} \right\} \quad (60)$$

$$|\kappa_{i,1}| \leq \min \left\{ \sqrt{\frac{2\iota}{(1 - \varpi_0)\mu_1}}, \sqrt{2 \left(\frac{\iota}{(1 - \varpi_0)\mu_2} \right)^{\frac{2}{1+\gamma}}} \right\} \quad (61)$$

within finite time $T_i = \max\{(2/(\varpi_0\mu_1(1 - \gamma))) \ln((\varpi_0\mu_1 V^{\frac{1-\gamma}{2}}(0) + \mu_2)/\mu_2), (2/(\mu_1(1 - \gamma))) \ln((\mu_1 V^{\frac{1-\gamma}{2}}(0) + \varpi_0\mu_2)/\varpi_0\mu_2)\}$. For $t \geq T_i$, $\chi_{i,1}$ finally enters into the following region

$$\begin{aligned} |\chi_{i,1}| &\leq |v_{i,1}| + |\kappa_{i,1}| \\ &\leq \min \left\{ 2\sqrt{\frac{2\iota}{(1 - \varpi_0)\mu_1}}, 2\sqrt{2 \left(\frac{\iota}{(1 - \varpi_0)\mu_2} \right)^{\frac{2}{1+\gamma}}} \right\}. \end{aligned} \quad (62)$$

From (62), the tracking error $\chi_{i,1}$ can be regulated arbitrarily small in finite time by choosing the appropriate design parameters. ■

V. SIMULATION RESULTS

In this section, a simulation example is carried out to show the effectiveness of the proposed finite-time adaptive trajectory tracking control scheme. The model parameters of quadrotor UAV are shown in TABLE 1.

TABLE 1. Model parameters.

Parameter values	
Model parameters	$m = 2\text{kg}, g = 9.8\text{m/s}^2, \ell = 0.325\text{m},$
	$J_x = 0.082\text{kg} \cdot \text{m}^2, J_y = 0.082\text{kg} \cdot \text{m}^2,$
	$J_z = 0.149\text{kg} \cdot \text{m}^2,$
	$G_x = G_y = G_z = 0.6\text{kg/s},$
	$G_\phi = G_\theta = G_\psi = 0.6\text{kg/rad},$
	$d_i = 2 \sin(0.2t) - \cos(0.2t + 0.2), i = 1, 2, 3,$
	$d_i = \sin\left(\frac{\pi}{15}t\right), i = 4, 5, 6.$

In the simulation, the desired position trajectories are given as $x_d = \sin\left(\frac{\pi}{15}t\right)$, $y_d = \cos\left(\frac{\pi}{15}t\right)$, $z_d = \frac{1}{6}t$, and the expected yaw angle is selected as $\psi_d = \frac{\pi}{4}$. The initial condition of the quadrotor UAV is chosen as $[\phi(0), \theta(0), \psi(0), x(0), y(0), z(0)] = [0, 0, 0, 0.8, 0.2, 0]$. The design parameters of the actual controllers, virtual control signals, parameter update laws and the finite-time command filters are provided in TABLE 2.

TABLE 2. Design parameters.

Parameter values	
Design parameters	$c_{1,1} = c_{2,1} = 2, c_{1,2} = c_{2,2} = 3,$
	$c_{3,1} = 4, c_{3,2} = 6, c_{4,1} = 3, c_{4,2} = 4,$
	$c_{5,1} = c_{6,1} = 6, c_{5,2} = c_{6,2} = 8,$
	$\epsilon_1 = \epsilon_2 = \epsilon_3 = 2.778 \times 10^{-4},$
	$\epsilon_4 = \epsilon_5 = \epsilon_6 = 1.235 \times 10^{-4},$
	$l_i = 2, m_i = n_i = 0.01,$
	$s_{i,1} = s_{i,2} = h_{i,1} = h_{i,2} = 3,$
	$\sigma_i = r_i = \omega_i = 0.1,$
	$a_{i,1} = 8, a_{i,2} = 5, i = 1, \dots, 6.$

The simulation results are shown in Figs. 1–7. Fig. 1 shows the trajectory tracking curves of quadrotor UAV in 3-D space. The curves of the actual trajectories and the desired trajectories are shown in Figs. 2–3. It can be seen from Figs. 1–3 that the developed finite-time control strategy can faster and accurately track the desired trajectories. Figs. 4–5 show the curves of the parameter update laws $\hat{\Theta}_i$ and \hat{p}_i . Figs. 6–7 plot the trajectories of the control input τ_i and quantized output signal $q(\tau_i)$, respectively.

Finally, the comparative simulation between FTCFB control algorithm and CFB control scheme in [22] is used to show the merits of proposed finite-time control strategy. The design parameters of CFB control scheme are the same as FTCFB control algorithm except that $s_{i,1} = s_{i,2} = h_{i,1} = h_{i,2} = 0$. The simulation comparison results of position

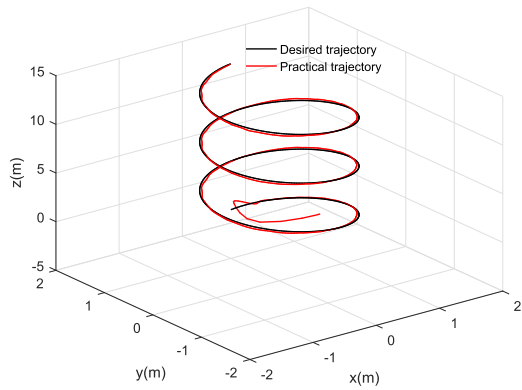


FIGURE 1. The curves of trajectory tracking in 3-D space.

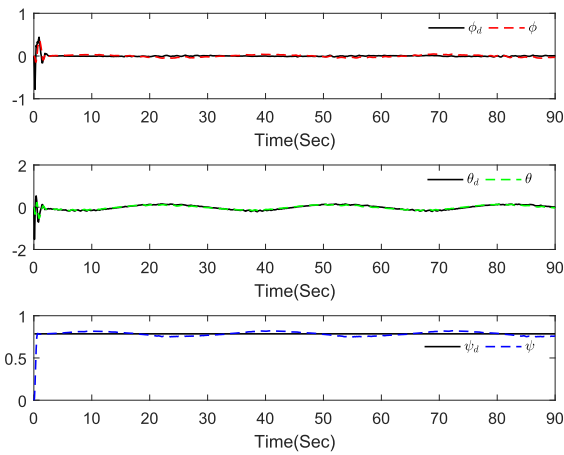


FIGURE 2. The curves of desired and actual states ϕ , θ and ψ .

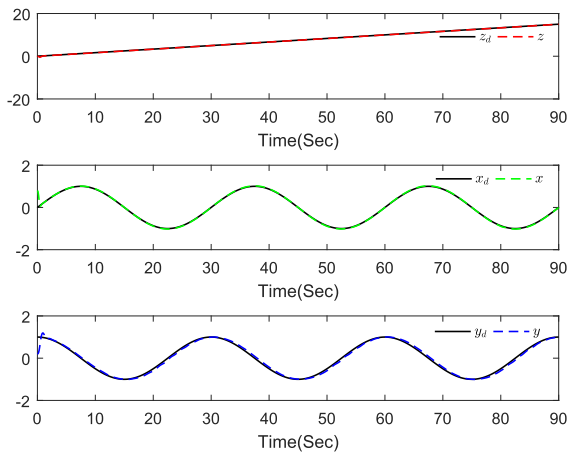


FIGURE 3. The curve of desired and actual states x , y and z .

and attitude tracking errors are shown in Figs. 8–9. From Figs. 8–9, it can be seen that the proposed FTCFB control algorithm can achieve desired performance with a smaller tracking error and a faster convergence speed. Nevertheless,

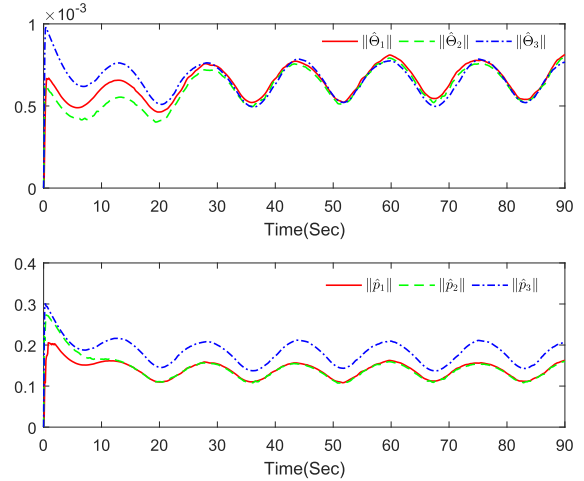


FIGURE 4. The curves of parameter update laws $\hat{\theta}_i$ and \hat{p}_i ($i = 1, 2, 3$).

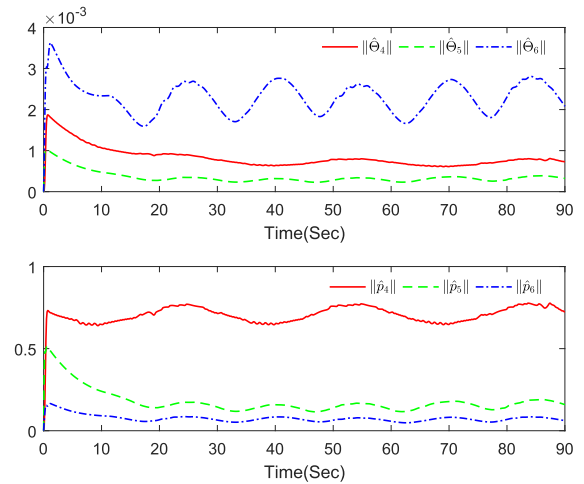


FIGURE 5. The curves of parameter update laws $\hat{\theta}_i$ and \hat{p}_i ($i = 4, 5, 6$).

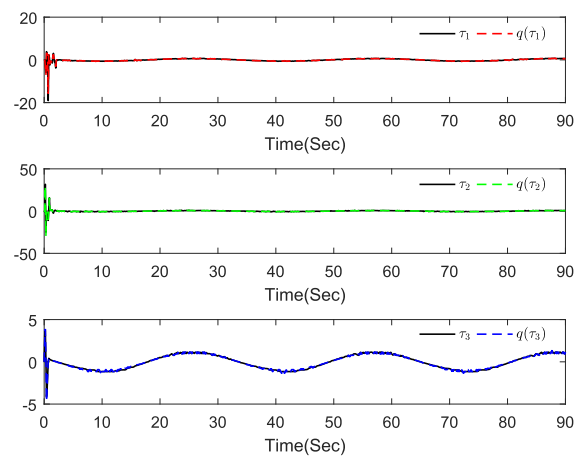


FIGURE 6. The curves of control input τ_i and quantized output signal $q(\tau_i)$ ($i = 1, 2, 3$).

there are still some shortcomings, such as relatively larger control energy and more design parameters, which will be improved in the future.

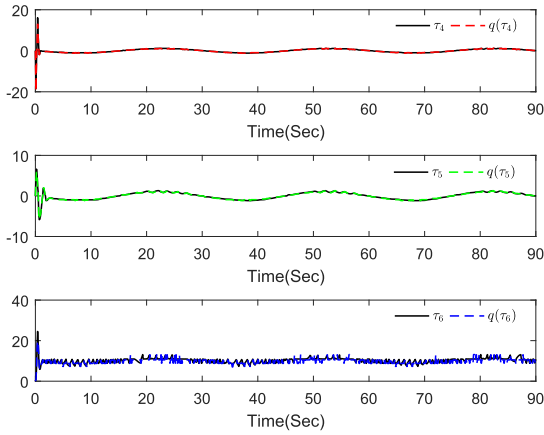


FIGURE 7. The curves of control input τ_i and its quantized output signal $q(\tau_i)$ ($i = 4, 5, 6$).

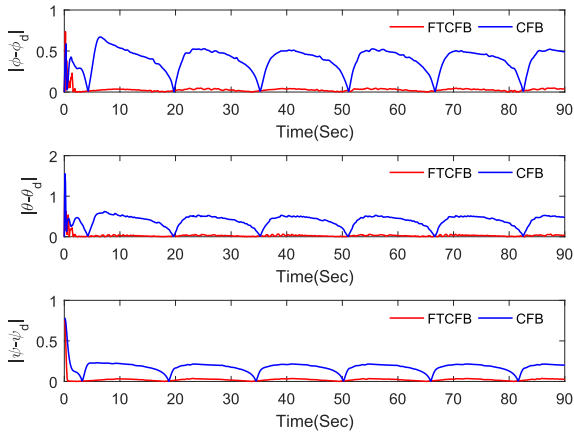


FIGURE 8. The curves of tracking errors of attitude subsystem.

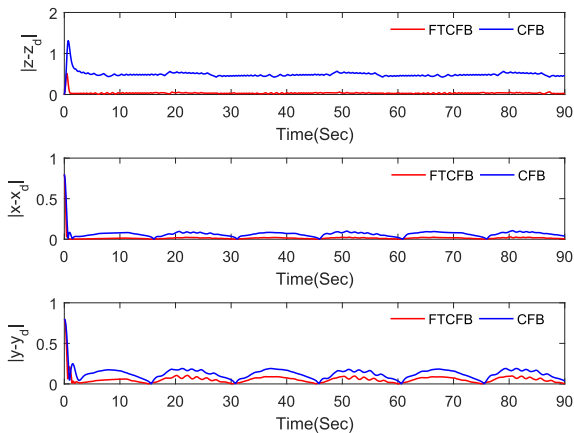


FIGURE 9. The curves of tracking errors of position subsystem.

VI. CONCLUSION

This paper has proposed a new FTFCFB adaptive quantized control scheme to solve trajectory tracking problem for a quadrotor UAV, which enables the finite-time convergence. The finite-time control algorithm has been designed for position subsystem and attitude subsystem via the CFB technique and finite-time control theory. Different from the previous results, the design does not need the priori information of quantization parameters associated with position subsystem

and attitude subsystem. Finally, a simulation example has confirmed the effectiveness of the developed finite-time control approach. Our future works will concentrate on the observer-based FTFCFB adaptive control for quadrotor UAV, as well as study the FTFCFB distributed consensus control for multiple quadrotor UAVs based on the results of [40] and [41].

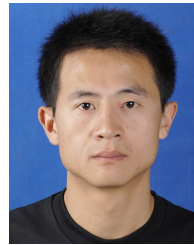
REFERENCES

- [1] L. Wang and J. Su, "Robust disturbance rejection control for attitude tracking of an aircraft," *IEEE Trans. Control Syst. Technol.*, vol. 23, no. 6, pp. 2361–2368, Nov. 2015.
- [2] W. Zhu, H. Du, Y. Cheng, and Z. Chu, "Hovering control for quadrotor aircraft based on finite-time control algorithm," *Nonlinear Dyn.*, vol. 88, no. 4, pp. 2359–2369, Feb. 2017.
- [3] S. Islam, P. X. Liu, and A. El Saddik, "Nonlinear adaptive control for quadrotor flying vehicle," *Nonlinear Dyn.*, vol. 78, no. 1, pp. 117–133, May 2014.
- [4] J. Zhang, D. Gu, Z. Ren, and B. Wen, "Robust trajectory tracking controller for quadrotor helicopter based on a novel composite control scheme," *Aerosp. Sci. Technol.*, vol. 85, pp. 199–215, Feb. 2019.
- [5] R. Xu and Ü. Özgüner, "Sliding mode control of a class of underactuated systems," *Automatica*, vol. 44, no. 1, pp. 233–241, Jan. 2008.
- [6] Y. Huang, Z. Zheng, L. Sun, and M. Zhu, "Saturated adaptive sliding mode control for autonomous vessel landing of a quadrotor," *IET Control Theory Appl.*, vol. 12, no. 13, pp. 1830–1842, Sep. 2018.
- [7] Y. Wang, X. Xie, M. Chadli, S. Xie, and Y. Peng, "Sliding mode control of fuzzy singularly perturbed descriptor systems," *IEEE Trans. Fuzzy Syst.*, early access, May 29, 2020, doi: 10.1109/TFUZZ.2020.2998519.
- [8] Q. Shen, Y. Shi, R. Jia, and P. Shi, "Design on type-2 fuzzy-based distributed supervisory control with backlash-like hysteresis," *IEEE Trans. Fuzzy Syst.*, early access, May 6, 2020, doi: 10.1109/TFUZZ.2020.2992864.
- [9] Y. Wang, C. K. Ahn, H. Yan, and S. Xie, "Fuzzy control and filtering for nonlinear singularly perturbed Markov jump systems," *IEEE Trans. Cybern.*, early access, Jul. 22, 2020, doi: 10.1109/TCYB.2020.3004226.
- [10] Q. Shen, P. Shi, R. K. Agarwal, and Y. Shi, "Adaptive neural network-based filter design for nonlinear systems with multiple constraints," *IEEE Trans. Neural Netw. Learn. Syst.*, early access, Jul. 28, 2020, doi: 10.1109/TNNLS.2020.3009391.
- [11] F. Chen, R. Jiang, K. Zhang, B. Jiang, and G. Tao, "Robust backstepping sliding-mode control and observer-based fault estimation for a quadrotor UAV," *IEEE Trans. Ind. Electron.*, vol. 63, no. 8, pp. 5044–5056, Aug. 2016.
- [12] N. Fethalla, M. Saad, H. Michalska, and J. Ghommam, "Robust observer-based dynamic sliding mode controller for a quadrotor UAV," *IEEE Access*, vol. 6, no. 45, pp. 846–859, Aug. 2018.
- [13] L. Xu, H. Ma, D. Guo, A. Xie, and D. Song, "Backstepping sliding-mode and cascade active disturbance rejection control for a quadrotor UAV," *IEEE/ASME Trans. Mechatronics*, early access, Apr. 27, 2020, doi: 10.1109/TMECH.2020.2990582.
- [14] C.-C. Hua, K. Wang, J.-N. Chen, and X. You, "Tracking differentiator and extended state observer-based nonsingular fast terminal sliding mode attitude control for a quadrotor," *Nonlinear Dyn.*, vol. 94, no. 1, pp. 343–354, Jun. 2018.
- [15] D. Swaroop, J. K. Hedrick, P. P. Yip, and J. C. Gerdes, "Dynamic surface control for a class of nonlinear systems," *IEEE Trans. Autom. Control*, vol. 45, no. 10, pp. 1893–1899, Oct. 2000.
- [16] W. A. Butt, L. Yan, and K. Amezquita S., "Adaptive integral dynamic surface control of a hypersonic flight vehicle," *Int. J. Syst. Sci.*, vol. 46, no. 10, pp. 1717–1728, Aug. 2013.
- [17] X. Shao, J. Liu, H. Cao, C. Shen, and H. Wang, "Robust dynamic surface trajectory tracking control for a quadrotor UAV via extended state observer," *Int. J. Robust Nonlinear Control*, vol. 28, no. 7, pp. 2700–2719, May 2018.
- [18] C. Fu, W. Hong, H. Lu, L. Zhang, X. Guo, and Y. Tian, "Adaptive robust backstepping attitude control for a multi-rotor unmanned aerial vehicle with time-varying output constraints," *Aerosp. Sci. Technol.*, vol. 78, pp. 593–603, Jul. 2018.

- [19] C. Hua, J. Chen, and X. Guan, "Dynamic surface based tracking control of uncertain quadrotor unmanned aerial vehicles with multiple state variable constraints," *IET Control Theory Appl.*, vol. 13, no. 4, pp. 526–533, Mar. 2019.
- [20] Z. Shen, F. Li, X. Cao, and C. Guo, "Prescribed performance dynamic surface control for trajectory tracking of quadrotor UAV with uncertainties and input constraints," *Int. J. Control*, early access, Mar. 6, 2020, doi: 10.1080/00207179.2020.1743366.
- [21] J. A. Farrell, M. Polycarpou, M. Sharma, and W. Dong, "Command filtered backstepping," *IEEE Trans. Autom. Control*, vol. 54, no. 6, pp. 1391–1395, Jun. 2009.
- [22] W. Dong, J. A. Farrell, M. M. Polycarpou, V. Djapic, and M. Sharma, "Command filtered adaptive backstepping," *IEEE Trans. Control Syst. Technol.*, vol. 20, no. 3, pp. 566–580, May 2012.
- [23] J. Yu, P. Shi, W. Dong, and H. Yu, "Observer and command-filter-based adaptive fuzzy output feedback control of uncertain nonlinear systems," *IEEE Trans. Ind. Electron.*, vol. 62, no. 9, pp. 5962–5970, Sep. 2015.
- [24] Z. Zuo, "Trajectory tracking control design with command-filtered compensation for a quadrotor," *IET Control Theory Appl.*, vol. 4, no. 11, pp. 2343–2355, Nov. 2010.
- [25] C. Hu, Z. Zhang, X. Zhou, and N. Wang, "Command filter-based fuzzy adaptive nonlinear sensor-fault tolerant control for a quadrotor unmanned aerial vehicle," *Trans. Inst. Meas. Control*, vol. 42, no. 2, pp. 198–213, Jan. 2020.
- [26] Y. C. Wang, W. S. Chen, S. X. Zhang, J. W. Zhu, and L. J. Cao, "Command-filtered incremental backstepping controller for small unmanned aerial vehicles," *J. Guid., Control, Dyn.*, vol. 41, no. 4, pp. 954–967, Apr. 2018.
- [27] A. Abouonia, A. El-Badawy, and R. Rashad, "Active anti-disturbance control of a quadrotor unmanned aerial vehicle using the command-filtering backstepping approach," *Nonlinear Dyn.*, vol. 90, no. 1, pp. 581–597, Jul. 2017.
- [28] L. Cao, Y. Wang, S. Zhang, and T. Fei, "Command-filtered sensor-based backstepping controller for small unmanned aerial vehicles with actuator dynamics," *Int. J. Syst. Sci.*, vol. 49, no. 16, pp. 3365–3376, Nov. 2018.
- [29] J. Zhou, C. Wen, and G. Yang, "Adaptive backstepping stabilization of nonlinear uncertain systems with quantized input signal," *IEEE Trans. Autom. Control*, vol. 59, no. 2, pp. 460–464, Feb. 2014.
- [30] C. Wang, C. Wen, Y. Lin, and W. Wang, "Decentralized adaptive tracking control for a class of interconnected nonlinear systems with input quantization," *Automatica*, vol. 81, pp. 359–368, Jul. 2017.
- [31] Z. Liu, F. Wang, Y. Zhang, and C. L. Philip Chen, "Fuzzy adaptive quantized control for a class of stochastic nonlinear uncertain systems," *IEEE Trans. Cybern.*, vol. 46, no. 2, pp. 524–534, Feb. 2016.
- [32] J. Hu, X. Sun, S. Liu, and L. He, "Adaptive finite-time formation tracking control for multiple nonholonomic UAV system with uncertainties and quantized input," *Int. J. Adapt. Control Signal Process.*, vol. 33, no. 1, pp. 114–129, Jan. 2019.
- [33] X. Zhang, Y. Wang, G. Zhu, X. Chen, Z. Li, C. Wang, and C.-Y. Su, "Compound adaptive fuzzy quantized control for quadrotor and its experimental verification," *IEEE Trans. Cybern.*, early access, May 14, 2020, doi: 10.1109/TCYB.2020.2987811.
- [34] J. Yu, P. Shi, and L. Zhao, "Finite-time command filtered backstepping control for a class of nonlinear systems," *Automatica*, vol. 92, pp. 173–180, Jun. 2018.
- [35] X. Zhang, "Lyapunov-based fault tolerant control of quadrotor unmanned aerial vehicles," Ph.D. dissertation, School Eng. Comput. Sci., Concordia Univ., Montreal, QC, Canada, 2010.
- [36] L. Wang, *Adaptive Fuzzy Systems and Control, Design and Stability Analysis*. Englewood Cliffs, NJ, USA: Prentice-Hall, 1994.
- [37] C. Qian and W. Lin, "A continuous feedback approach to global strong stabilization of nonlinear systems," *IEEE Trans. Autom. Control*, vol. 46, no. 7, pp. 1061–1079, Jul. 2001.
- [38] G. H. Hardy, J. E. Littlewood, and G. Pólya, *Inequalities*. Cambridge, U.K.: Cambridge Univ. Press, 1952.
- [39] G. Cui, J. Yu, and Q.-G. Wang, "Finite-time adaptive fuzzy control for MIMO nonlinear systems with input saturation via improved command-filtered backstepping," *IEEE Trans. Syst., Man, Cybern. Syst.*, early access, Aug. 6, 2020, doi: 10.1109/TSMC.2020.3010642.
- [40] Q. Shen, P. Shi, J. Zhu, and L. Zhang, "Adaptive consensus control of leader-following systems with transmission nonlinearities," *Int. J. Control*, vol. 92, no. 2, pp. 317–328, Feb. 2019.
- [41] Q. Shen, P. Shi, J. Zhu, S. Wang, and Y. Shi, "Neural networks-based distributed adaptive control of nonlinear multiagent systems," *IEEE Trans. Neural Netw. Learn. Syst.*, vol. 31, no. 3, pp. 1010–1021, Mar. 2020.

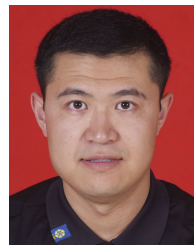


WEI YANG is currently pursuing the M.Sc. degree with the School of Electronic and Information Engineering, Suzhou University of Science and Technology. His research interests include intelligent control of quadrotor UAV and adaptive control of nonlinear systems.



GUOZENG CUI received the B.Sc. degree in applied mathematics from the Shandong University of Technology, Zibo, China, in 2009, the M.Sc. degree in applied mathematics from Qufu Normal University, Qufu, China, in 2012, and the Ph.D. degree in control science and engineering from the Nanjing University of Science and Technology, Nanjing, China, in 2016.

He is currently a Lecturer with the School of Electronic and Information Engineering, Suzhou University of Science and Technology. His research interests include adaptive control, intelligent control for nonlinear systems, and multi-agent systems.



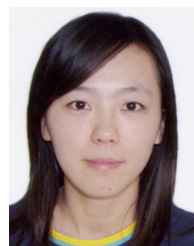
JINPENG YU received the B.Sc. degree in automation from Qingdao University, Qingdao, China, in 2002, the M.Sc. degree in system engineering from Shandong University, Jinan, China, in 2006, and the Ph.D. degree in system theory from the Institute of Complexity Science, Qingdao University, in 2011.

He is currently a Distinguished Professor with the School of Automation, Qingdao University. His research interests include electrical energy conversion and motor control, applied nonlinear control, and intelligent systems. He was a recipient of the Shandong Province Taishan Scholar Special Project Fund and the Shandong Province Fund for Outstanding Young Scholars.



CHONGBEN TAO received the B.Sc. and Ph.D. degrees from Jiangnan University, Wuxi, China.

He is currently a Lecturer with the School of Electronic and Information Engineering, Suzhou University of Science and Technology. His current research interests include deep learning, vision SLAM, semantic mapping, and embedded systems.



ZELI (Member, IEEE) received the B.Sc. degree in electronic information engineering and the Ph.D. degree in control science and engineering from the Nanjing University of Science and Technology, Nanjing, China, in 2005 and 2010, respectively.

She is currently an Associate Professor with the School of Electronic and Information Engineering, Suzhou University of Science and Technology. Her research interests include robust control and filtering, time-delay systems, stochastic systems, nonlinear systems, and fuzzy systems.

• • •